Ab Initio Determination of the Force Field of Dichloromethane, Verified by Gas-Phase Infrared Frequencies and Intensities and Applied to a Combined Electron Diffraction and Microwave Investigation of Geometry

Y. Wang, J. Tremmel,† J. De Smedt, C. Van Alsenoy, and H. J. Geise*

University of Antwerp (UIA), Department of Chemistry, Universiteitsplein 1, B-2610 Wilrijk, Belgium

B. Van der Veken

University of Antwerp (RUCA), Department of Inorganic Chemistry, Groenenborgerlaan 171, B-2020 Antwerp, Belgium

Received: February 26, 1997; In Final Form: June 11, 1997[⊗]

For CH_2Cl_2, using 6-31G*/66-31G* basis sets, the complete geometry-relaxed force field and the dipole moment derivatives along internal coordinates were calculated. The study of the force field scaling procedure yielded (i) agreement with experimental IR frequencies with a root mean square deviation of 9.6 cm^{-1} and maximum deviation of 18 cm^{-1}, (ii) guidelines to select the number of scale factors and the way symmetry coordinates should be distributed over the scale factor groups, and (iii) the recognition that deviations of the scale factors from unity may be used to measure the performance of the basis set. Absolute IR band intensities were calculated and had the same sequence as the gas-phase intensities. Ab initio intensity calculations may thus become a valuable tool in the assignment of IR spectra. For example, it was proved that the 1467 cm^{-1} band is not the CH_2-scissoring mode. Furthermore, support was found for the model of Evans and Lo, rationalizing the remarkable intensity changes of inter alia the symmetric and asymmetric CH_2 stretches induced by environmental changes. From a joint analysis of electron diffraction and microwave data the following r_α^0 parameters were obtained, r(C−Cl) = 1.772(2) Å, r(C−H) = 1.090(10) Å; ∠Cl−C−Cl = 112.0(1)°; ∠HCH = 112(1)°. Comparison—on a r_α^0 basis—with other CCl bond lengths in the series $CH_{4-n}Cl_n$ (n = 1−4) shows the competition of two effects, a shortening caused by electronegativity and a lengthening caused by steric hindrance. We consider the estimated uncertainties of the ab initio calculated electron diffraction thermal parameters smaller than the experimental errors.

Introduction

The many (empirical) relations used in chemistry[1] that contain force constants bear witness to the fact that the force field of a molecule is the key to many important molecular quantities, such as vibrational constants, thermal amplitudes and bond parameters. The determination of a complete force field has been and still is a challenge, even for a small symmetrical molecule. Due to the limited amount of data experimentally available, the off-diagonal force constants are extremely difficult to obtain. This is unfortunate, because they provide the information about the change in stiffness of a bond, resulting from the distortion of the other bonds.[2] Since we routinely calculate quadratic, harmonic force fields that allow us to calculate vibrational frequencies and to check their assignments,[3] we now wish to extend the procedure toward infrared intensities. Knowledge of band intensities is of great fundamental and practical importance because they are very sensitive to substitution and in general to changes in the molecular environment. Their study, however, lags behind frequency studies mainly because of technical limitations in measuring absolute band intensities.

We selected dichloromethane, CH_2Cl_2, as the test molecule because it has high symmetry (C_{2v}) and a significant part of its experimental force field is available for comparison. When Davis, Robiette, and Gerry reviewed[4] in 1981 the state-of-affairs concerning the CH_2Cl_2 force field, several force constants were missing. To the vibrational wavenumbers of Escribano et al.[5] were added the quartic centrifugal distortion constants of $^{12}CH_2{}^{35}Cl_2$ and $^{12}CD_2{}^{35}Cl_2$ by Davis et al. After an initial fit of the diagonal force constants using vibrational wavenumbers alone was obtained, the off-diagonal constants were gradually introduced with the inclusion of the distortion constants. The force field obtained in this elegant microwave work was greatly improved, most off-diagonal constants becoming more reliable in magnitude and sign. Yet, the four interaction constants between the CH stretching modes with the other modes were constrained to 0 during the refinements and hence remained indeterminate.

Therefore the aim of this work is 2-fold. With the help of ab initio calculations we want to produce for CH_2Cl_2 in the gas phase (i) a complete and reliable force field that settles some long standing questions about its IR behavior and (ii) a self-consistent molecular model that is simultaneously consistent with electron diffraction, microwave, and infrared data, including IR intensities.

Experimental Section

A commercial sample (Janssen Chimica) of dichloromethane (HPLC grade, 99.6% purity) was used.

Electron diffraction data were recorded photographically on the Antwerpen diffraction unit manufactured by Technisch Physische Dienst, TPD-TNO, Delft, The Netherlands. The nozzle temperature was kept at about 300 K. An accelerating voltage of 60 kV, stabilized within 0.01% during the measurements, was employed. The electron wavelength was calibrated against the known diffraction pattern of benzene,[6] resulting in

* Author to whom correspondence should be addressed.
† Visiting professor from Department of Structural Chemistry, Hungarian Academy of Science, Eötvös University, Budapest, Hungary.
⊗ Abstract published in *Advance ACS Abstracts,* August 1, 1997.

S1089-5639(97)00719-6 CCC: $14.00

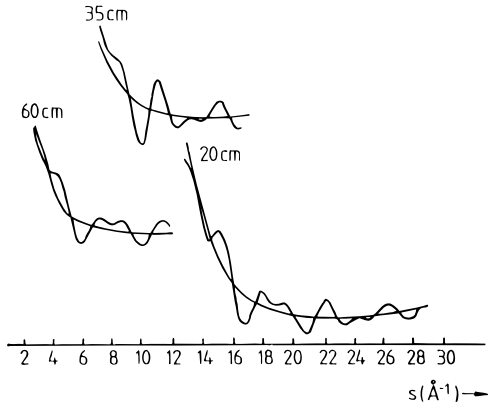

Figure 1. Experimental leveled intensities, $I(s)$, with final backgrounds, $B(s)$, for CH_2Cl_2.

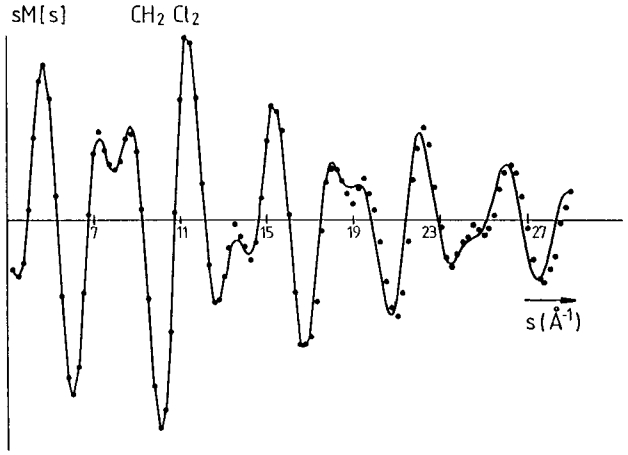

Figure 2. Experimental (●) and theoretical (—) sM (s) curve for CH_2Cl_2.

$\lambda = 0.048\,614\,(2)$ Å. Four plates (Kodak electron image) were selected from recordings taken at the nozzle-to-plate distance of 600.05(2) mm, four plates from the distance of 350.04(2) mm, and five plates from the distance of 200.05(2) mm. Optical densities were measured on a modified, microprocessor-controlled, rotating Elscan E-2500 microdensitometer.[7] Optical density values were converted to intensities by using the one-hit model of Forster.[8]

Coherent scattering factors were taken from Bonham and Schäfer[9] and incoherent scattering factors from Tavard et al.[10] The data was further processed by standard procedures.[11] Leveled intensities were obtained in the following regions, all with $\Delta s = 0.25$ Å^{-1}: 60 cm, $3.25 \le s \le 12.00$ Å^{-1}; 35 cm, $7.50 \le s \le 17.00$ Å^{-1}; 20 cm, $13.00 \le s \le 29.00$ Å^{-1}. Leveled intensities with final backgrounds and the combined molecular intensities (sM(s) curve) are shown in Figures 1 and 2, respectively.

Gas-phase IR spectra were recorded at room temperature (295 K) on a Bruker IFS 66v Fourier transform infrared spectrometer using a globar source, a KBr/Ge beamsplitter and a broad band MCT detector. Low-pressure vapors were contained in a 20 cm gas cell sealed with KBr windows. Pressure broadening experiments were performed in a 7 cm cell equipped with either CaF_2 or wedged Si windows. Interferograms were averaged over 200 scans, Happ Genzel apodized, and Fourier transformed using a zero-filling factor of 8 to obtain spectra at a resolution of 0.5 cm^{-1}. Vapor pressures of dichloromethane were measured using a capacitance manometer.

It is worth noting that in the CH_2 scissors region a band of rather complicated profile occurs, centered at $\nu = 1467$ cm^{-1}. This band was also observed by Saeki and Tanabe[12] who suggested that it does not represent the gas-phase value of the CH_2 scissors mode but might be assigned to an overtone or combination band, irrespective of its rather high intensity. We will show below that our calculations strongly support this view. The true CH_2 scissors band, unambiguously corresponding to the A_1 species, is found[5,13] in the gas-phase Raman spectrum of CH_2Cl_2 at $\nu_3 = 1434$ cm^{-1}. Now, a comparison between our frequencies and those of Escribano et al.[5] shows that they are within experimental error with a root mean square (rms) deviation of 2.6 cm^{-1} and a maximum deviation of 5 cm^{-1}.

The spectra were recorded on an absorbance scale to allow for a direct comparison of experiments and calculations. Experimental vibrational band absorbancies, A, were determined as

$$A = \frac{1}{cl}\int \ln\frac{I_0}{I}\,\mathrm{d}\nu = \frac{1}{cl}\sum_i \left(\ln\frac{I_0}{I}\right)_i \Delta\nu_i \qquad (1)$$

Here, c is the molar concentration or gas pressure, l the path length through the sample, I_0 and I are the intensities of the incoming and outgoing beam, respectively, and ν the frequency. Strictly speaking, the intensity A as defined above gives the apparent band intensity, and the absolute band intensity should be obtained by extrapolating to $cl = 0$. In this case, as in many other cases,[12] the extrapolation was omitted. Previously, Saëki et al.[12] measured the IR intensities of CH_2Cl_2 using gas cells of 5 and 10 cm path length and pressures between 7.5 and 375 hPa. We followed their approach, but used a longer gas cell (20.8 cm) and lower pressures (4.2 and 5−6 hPa). We believe that the latter pressures are low enough to be sure of linear intensity−pressure conditions, except perhaps for the most intense band, the asymmetric C−Cl stretch.

At the resolution used, the type B and C bands, of symmetry A_1 and B_1, respectively, show rather extensive rotational fine structure. Problems with the integration of these bands were avoided by using pressure broadening. In samples pressurized with 15 bar of argon, the rotational fine structure completely disappeared, and measurements were performed at that pressure. It was found that for the pressure-broadened spectra the concentration of dichloromethane was difficult to establish, and consequently, the following procedure for the determination of integrated intensities had to be adopted. The type A bands show no rotational fine structure, and their intensity can be reliably measured even at low pressures. The well-isolated type A band at 1270 cm^{-1} was chosen as the internal standard. Its intensity was determined at a vapor pressure of 10 mbar by integrating the spectrum between 1325 and 1200 cm^{-1}. From the pressure-broadened spectra the intensities of the fundamentals were determined relative to that of the 1270 cm^{-1} band. Using the above low-pressure intensity of the latter, they were transformed into absolute intensities. Wherever possible, the frequency interval in which integration was performed was chosen to be sufficiently wide to ensure that the wing intensities were properly taken into account. Overlap of a fundamental either by another fundamental or by other transitions in the spectrum occurs for the CH_2 stretches at 3068 and 2997 cm^{-1}, for the CCl_2 stretches at 760 and 715 cm^{-1}, and for the CH_2 scissoring at 1434 cm^{-1}. The intensity of the 1434 cm^{-1} band and that of the weaker component in each of the two fundamental doublets was estimated as twice the integral from the band center outward, i.e. away from the overlap. The values obtained in this way must be regarded as upper limits. For the CH_2 and CCl_2 stretches the sum intensity of the doublet was also measured. The intensity of the 3068 cm^{-1} band is more than two orders of magnitude smaller than that of the 2997 cm^{-1}

TABLE 1: Ab Initio Optimized Geometries (r_e type) for Dichloromethane

	4-21G*/33-21G* basis set	6-31G*/66-31G* basis set
C−H (Å)	1.071	1.079
C−Cl (Å)	1.788	1.777
H−C−H (deg)	111.8	110.9
Cl−C−Cl (deg)	111.6	112.9
H−C−Cl (deg)	108.4	108.3
$-E$ (hartree)	953.563 87	957.950 87
$-E$ (kcal/mol)	598 370.22	601 123.11
largest residual force (mdyn)	0.0006	0.0001
dipole moment (D)	2.08	1.98

band; therefore, the sum intensity of the doublet was taken to be the intensity of the dominant band. For the CCl_2 stretches, the intensity of the dominant component at 760 cm^{-1} was obtained as the difference between the sum intensity and the above weaker component. As the presumably somewhat overestimated intensity of the weaker component is a mere 9% of that of the stronger component, this approximation should not cause a significant error in the intensity of the latter.

Theoretical Models and Vibrational Spectroscopy

Pulay's ab initio gradient method[14,15] and the program BRABO[16] were used to perform the geometry optimizations. At first we employed a 4-21G* basis set[17] on C and H atoms with a 33-21G* set[18,19] on Cl and later the larger 6-31G* basis set[20,21] on C and H with a 66-31G* set[18,19] on Cl. Geometries were considered converged when the largest residual force on each atom was less than 10^{-3} mdyn. The results are given in Table 1. Comparing the results of the 4-21G* and the 6-31G* calculations, one notes, as expected, some differences in the numerical values. For example, the overestimation of the C−Cl bond length and the molecular dipole moment, due to deficiencies in the basis sets, is diminished by using the larger 6-31G* basis set. Also, the ClCCl valence has increased by 1.3°, and the HCH angle decreased by 0.9°.

Using the 6-31G*/66-31G* basis set, we then calculated the harmonic quadratic force field of dichloromethane by applying a two-sided curvilinear distortion[17] to each internal coordinate from its equilibrium geometry. Displacements of ±0.01 Å for bond lenghts and of ±0.04 rad for valence angles were made. For each of these distorted geometries the dipole moment and the forces on the internal coordinates were determined. Force constants F_{ij} follow from

$$F_{ij} = \frac{\phi_j(q_i - \Delta_i) - \phi_i(q_i + \Delta_i)}{2\Delta_i} \qquad (2)$$

where ϕ_j denotes the force acting along internal coordinate q_j and Δ_i is the displacement along q_i. In this way the full set of diagonal (F_{ii}) and off-diagonal (F_{ij}) constants is obtained simultaneously. It is well known that, partly due to neglect of electron correlation and partly due to basis set truncation, ab initio self-consistent field methods systematically overestimate the force constants. They are scaled down using the linear scaling formula

$$F_{ij}(\text{scaled}) = F_{ij}(\text{unscaled})\ (\alpha_i\alpha_j)^{1/2}$$

in which α_i denotes the scale factor belonging to the internal coordinate q_i.[22,23] The α_i values are calculated, after defining local symmetry coordinates S_j in terms of the internal coordinates q_i (see Table 2 and Figure 3), by fitting the calculated vibrational frequencies onto assigned, experimental gas-phase IR frequencies.

It should be noted that our definitions of symmetry coordinates (Table 2) differ from those of Davis et al.[4] at S_5, S_7, and S_8 by a change in sign. More importantly S_1 and S_3 differ in that the latter authors defined S_3 as $m\theta(4,1,5) - n\{\theta(2,1,4) + \theta(2,1,5) + \theta(3,1,4) + \theta(3,1,5)\}$, with $m = 0.89$ and $n = 0.22$. That is, S_3 is a pure ClCCl bending coordinate with no accompanying change in the HCH valence angle. The coefficients m and n were calculated from the assumed geometry to remove the first-order redundancy between the six valence angles and to normalize S_3. The authors defined S_1 in a similar way as a pure HCH bending coordinate with no accompanying change in the ClCCl angle. Their subsequent force field analysis, however, yielded a strong bend−bend interaction constant. Bend−bend interactions (i.e. scissoring modes) are introduced naturally using standard projection operators[24] leading in this case to $s_3 = 2\theta(4,1,5) - \theta(2,1,4) - \theta(2,1,5) - \theta(3,1,4) - \theta(3,1,5) + 2\theta(2,1,3)$ and $s_1 = \theta(4,1,5) - \theta(2,1,3)$. Note that the ratio $m/n = 2$ results from the removal of degeneracy and contains no normalization. We started from this point and took $S_1 = s_1 + s_3$ and $S_3 = s_1 - s_3$. This emphasizes the fact that these symmetry coordinates describe scissoring modes and that a displacement in the ClCCl angle is accompanied by a smaller displacement in the HCH angle and vice versa. Furthermore, it was found (see below) that now S_1 and S_3 account almost completely for the vibrations at $\nu_1 = 282$ cm^{-1} and $\nu_3 = 1434$ cm^{-1}, respectively.

The number of scale factors α_i and the way the S_i are distributed over the scale factor groups should reflect the fact that the α_i are called into existence to counteract the systematic errors in the computations, particularly the deficiencies in the basis set and the omission of electron correlation. If our force field calculations with the 6-31G*/66-31G* basis set would have the same systematic errors (i.e. similar in magnitude) for all atoms and all vibrational modes, then one α should be sufficient. In another, less optimistic approximation, the deficiencies for stretching constants may be different from those for bending constants, and the deficiences for constants involving Cl atoms may differ from those involving C and H atoms. This reasoning limits the number of α_i to a maximum of four, and helps to select groups of S_i in a systematical way. Thus, we divided the S_i into four categories: (A) Cl stretchings, S_2, S_6; (B) H stretchings, S_4, S_9; (C) dominantly Cl bendings, S_1, and (D) dominantly H bendings, S_3. The coordinates S_5, S_7, and S_8 may be placed in either category C or category D, but should be kept together. This reasoning led to 19 scale factor groupings, some of which are obviously intuitively more logical than others. Nevertheless, for each of them the fitting of calculated frequencies onto experimental ones was performed; Table 3 gives the results. To discriminate among the 19 runs, one may compare the ratio of the R values ($R = \{\sum_i[\nu_i(\text{obs}) - \nu_i(\text{calc})]^2/\sum_i\nu_i(\text{obs})^2\}^{1/2}$) of two such groupings with tabulated[25] values of $P(p,n-p,\alpha)$, in which p denotes the degrees of freedom (here number of frequencies) and α the chosen level of significance. If the ratio is larger than P, then one rejects the hypothesis that the two runs are equal in performance at the 100α% significance level.

Executing the test at the 10% level of significance one can not distinguish between the runs VII, IX, XV, XVII, XVIII, and XIX, but one may reject the others. We conclude that three scale factors are sufficient and that neither S_1 nor S_3 should be treated separately. Further inspection suggests (albeit not statistically significant) to group S_3 with S_5, S_7, and S_8. The three remaining runs lead to quasi-equal scale factors, although run IX performs slightly better than VII and XVII. Hence, we grouped S_1 together with S_2 and S_6. It is gratifying that the

TABLE 2: Definition of Symmetry Coordinates S_i in Terms of Internal Coordinates[a]

	symmetry species	combination of internal coordinates[b]	description
S_1	A_1	$\theta(2,1,3) - \theta(2,1,4) - \theta(3,1,4) + 3\theta(4,1,5) - \theta(2,1,5) - \theta(3,1,5)$	C−Cl_2 scissors
S_2	A_1	$r(1,4) + r(1,5)$	C−Cl symm stretch
S_3	A_1	$3\theta(2,1,3) - \theta(2,1,4) - \theta(3,1,4) + \theta(4,1,5) - \theta(2,1,5) - \theta(3,1,5)$	CH_2 scissors
S_4	A_1	$r(1,2) + r(1,3)$	C−H symm stretch
S_5	A_2	$\theta(2,1,4) - \theta(3,1,4) - \theta(2,1,5) + \theta(3,1,5)$	twist
S_6	B_2	$r(1,4) - r(1,5)$	C−Cl asymm stretch
S_7	B_2	$\theta(2,1,4) - \theta(2,1,5) + \theta(3,1,4) - \theta(3,1,5)$	CH_2 wagging ≡ C Cl_2 rocking
S_8	B_1	$\theta(2,1,4) - \theta(3,1,4) + \theta(2,1,5) - \theta(3,1,5)$	CH_2 rocking ≡ C Cl_2 wagging
S_9	B_1	$r(1,2) - r(1,3)$	C−H asymm stretch

[a] See Figure 3 for numbering of atoms. [b] $r(i,j)$ signifies a bond distance between atoms i and j; $\theta(i,j,k)$ signifies a valence angle between atoms i, j, and k.

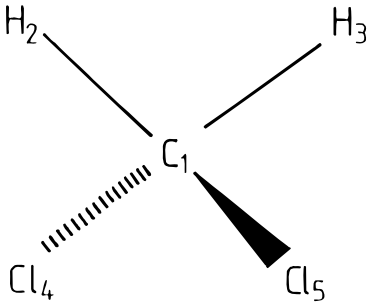

Figure 3. Atomic numbering scheme.

above statistical approach produces a distribution of S_i over three scale factor groups as well as numerical values of scale factors which reflect some well-known facts, i.e. the 6-31G* basis set performs (i) particularly well for Cl-related properties and (ii) better for stretching than for bending modes. In fact, we believe that the deviation of α_i from unity may be regarded as a useful measure of basis set performance.

The best scaled force field is presented in Table 4, while Table 5 shows the comparison between calculated and observed frequencies. Four points may be noted here. First, the experimental frequencies are excellently reproduced: the root mean square and largest deviation are only 9.6 and 18 cm^{-1}, respectively. Second, the assignments based on the $\mathbf{L}^{-1}$ matrix show that our definitions (Table 2) lead to an almost perfect one-to-one relation between S_i and ν_i (about 100% localization) and that in contrast to Davis et al.[4] a significant interaction constant is no longer needed between S_1 and S_3. Third, the off-diagonal force constants F_{14}, F_{24}, F_{34}, and F_{89}, indeterminate in earlier work, are now determined. As stated in the Introduction, they represent the interaction between the CH stretchings with the other modes. It is found that F_{34}, the interaction between the symmetric CH stretching and the CH_2 scissoring, is significant and non-negligible. This phenomenon is reasonable because the frequencies involved belong to the same A_1 symmetry species and are not too far apart. Fourth, the following rationalization, based on simple valence arguments and known IR behavior, can be used to give all the signs and almost all relative magnitudes of the interaction constants. When a C−X bond is lengthened in the molecule X_2CY_2, the electron rearrangement in the C−X part is obviously accompanied by an electron rearrangement in the XCY_2 part and the C atom tends toward an sp^2 hybridization. Electronegativity differences predict that for X = Cl the rearrangements will be more extensive than those for X = H. Thus, $|F_{12}|$, $|F_{23}|$, and $|F_{67}|$ must be and are larger than $|F_{14}|$, $|F_{34}|$, and $|F_{89}|$. Furthermore, the shift toward sp^2 hybridization upon lengthening of C−X stiffens the C−Y bonds as well as the XCX and XCY angles but softens the YCY angle. Thus F_{24}, F_{12}, F_{34}, F_{67}, and F_{89} must be positive, whereas F_{14} and F_{23} must be negative. Since CCl_2 and CH_2 scissoring both involve XCX and YCY angle deformations, it is logical that the opening of one angle softens the other, i.e. F_{13} is negative as calculated.

Absolute band intensities A_j were calculated from[26]

$$A_j = \frac{N\pi}{3c^2}\left(\frac{\delta\mu}{\delta Q_j}\right)^2 \tag{3}$$

in which N is Avogadro's constant, c the speed of light, and $\delta\mu/\delta Q_j$ the derivative of the dipole moment μ with respect to the vibrational normal coordinate Q_j. The latter derivatives follow from

$$\frac{\delta\mu}{\delta Q_j} = \sum_i \frac{\delta\mu}{\delta q_i}\frac{\delta q_i}{\delta Q_j} \tag{4}$$

with

$$\frac{\delta\mu}{\delta q_i} = [\mu(q_i - \Delta_i) - \mu(q_i - \Delta_i)]/2\Delta_i \tag{5}$$

in which q_i and Δ_i are defined as in eq 1. The standard vibrational treatment using Wilson's GF matrix method[2] was employed to calculate $\delta q_i/\delta Q_j$. The resulting calculated intensities together with our experimental ones are given in Table 6. Comparing I(calc) and I(expt) on a relative scale, it can be seen that the sequence of I(calc) faithfully reproduces that of I(expt). On an absolute scale I(calc) has a tendency to overestimate the I(expt) by a factor of about 1.5. From this together with the fact that most of the fundamental band centers suffer from overlap (see Experimental Section) we estimate an upper limit of I(calc)/I(expt) of about 2.

This brings support to the suggestion of Saëki et al.[12] that the band observed at 1467 cm^{-1} in the gas phase does not represent the CH_2 scissors mode. Not only is the calculated scissoring frequency (1430 cm^{-1}, Table 5) very close to Saëki's suggested value, but the intensity of the 1467 cm^{-1} band also is 8 times larger than the intensity computed for the CH_2 scissors. This would constitute a deviation far outside the error limit if the 1467 cm^{-1} band would be the CH_2 scissors mode.

In 1965, Evans and Lo[28] proposed a model (henceforth abbreviated as the E&L model) which explains the solvent sensitivity of the IR bands and the remarkable difference between the symmetric and antisymmetric CH_2 stretching modes. The value of this model was later questioned.[12] Now, we believe we are able to provide arguments indicating that the E&L model has great, albeit qualitative, predicting power. The authors follow the classic approach to IR intensities (eqs 3−5) and consider the dipole moment as the resultant of bond moments. They then argue that an extension of the C−H bond changes the hybridization at carbon such that the orbital at H acquires more p character, while that directed at Cl necessarily acquires more s character. This causes the carbon to appear more negative to the Cl and thus decreases the C−Cl bond

TABLE 3: Definitions of Groups of Symmetry Coordinates S_i Used in the Scaling Experiments of the 6-31G*/66-31G* Force Field, Together with Resulting Scale Factors, rms Deviations, Maximum Deviations, and *R* Factors[a]

run	symmetry coordinates, S_i	scale factor	rms dev (cm^{-1})	max dev (cm^{-1})	*R* factor
I	1, 2, 3, 4, 5, 6, 7, 8, 9	0.815	22.4	42.6	0.0178
II	2, 6	0.913	13.7	23.1	0.0066
	1, 3, 4, 5, 7, 8, 9	0.815			
III	2, 6, 4, 9	0.816	20.1	43.6	0.0144
	1, 3, 5, 7, 8	0.793			
IV	2, 6, 1	0.908	13.6	23.2	0.0066
	3, 4, 5, 7, 8, 9	0.815			
V	3, 4, 9	0.816	23.7	49.4	0.0201
	1, 2, 5, 6, 7, 8	0.799			
VI	2, 3, 6	0.808	23.1	45.0	0.0190
	1, 4, 5, 7, 8, 9	0.815			
VII	2, 6	0.907	10.1	18.2	0.0036
	4, 9	0.816			
	1, 3, 5, 7, 8	0.795			
VIII	2, 6	0.902	14.5	23.4	0.0075
	1	0.978			
	4, 3, 5, 7, 8, 9	0.815			
IX	4, 9	0.816	9.6	18.2	0.0032
	3, 5, 7, 8	0.795			
	1, 2, 6	0.901			
X	1	1.268	21.0	31.4	0.0157
	3, 5, 7, 8	0.793			
	2, 4, 6, 9	0.816			
XI	2, 6, 4, 9	0.816	20.1	43.8	0.0146
	1, 5, 7, 8	0.790			
	3	0.798			
XII	1, 2, 5, 6, 7, 8	0.799	23.1	49.4	0.0190
	4, 9	0.816			
	3	0.797			
XIII	2, 3, 6	0.808	21.8	46.9	0.0170
	4, 9	0.816			
	1, 5, 7, 8	0.790			
XIV	2, 6	0.912	12.8	23.5	0.0059
	1, 4, 5, 7, 8, 9	0.815			
	3	0.799			
XV	2, 6	0.908	11.4	19.8	0.0047
	1, 5, 7, 8	0.792			
	3, 4, 9	0.816			
XVI	1	1.343	24.0	52.4	0.0205
	4, 9	0.816			
	2, 3, 5, 6, 7, 8	0.796			
XVII	2, 6	0.905	9.8	18.2	0.0034
	1, 4, 9	0.816			
	3, 5, 7, 8	0.795			
XVIII	2, 6	0.906	10.2	19.9	0.0037
	4, 9	0.816			
	3	0.799			
	1, 5, 7, 8	0.792			
IXX	2, 6	0.895	10.9	18.3	0.0042
	4, 9	0.816			
	1	0.982			
	3, 5, 7, 8	0.794			

[a] rms deviation, $\{\sum_i[\nu_i(\text{obs}) - \nu_i(\text{calc})]^2/(n-1)\}^{1/2}$; max deviation, max of $|\nu_i(\text{obs}) - \nu_i(\text{calc})|$ $i = 1, ..., 9$; *R* factor, $\{\sum_i[\nu_i(\text{obs}) - \nu_i(\text{calc})]^2/\sum_i[\nu_i(\text{obs})]^2\}^{1/2}$.

moment. Their reasoning boils down to the conclusion that $\delta\mu(C-H)/\delta r(C-H)$ has a very small positive value, whereas $\delta\mu(C-Cl)/\delta r(C-H)$ has a very large negative value. This conclusion is confirmed by our ab initio calculations and thus gives credibility to the underlying hybridization arguments, which in turn are used to predict the consequences of H-bond formation in liquid CH_2Cl_2 based on the intensities of the symmetric and antisymmetric CH_2 stretches. The success of the E&L model emphasizes the risks encountered when one extrapolates IR liquid (or solution) intensities to gas-phase intensities with the help of formulas that contain only the refractive index and/or the dielectric permittivity.[29-32] These risks are particularly high with molecules in which complexation leads to significant rearrangements of the electron distribution.

TABLE 4: Scaled 6-31G* Force Constants (in mdyn $Å^{-1}$, mdyn rad^{-1}, or mdyn Å) Based on Symmetry Coordinates Defined in Table 2

	S_1	S_2	S_3	S_4	S_5	S_6	S_7	S_8	S_9
S_1	1.072								
S_2	0.276	3.788							
S_3	−0.072	−0.309	0.553						
S_4	−0.007	0.080	0.115	5.040					
S_5	0	0	0	0	0.597				
S_6	0	0	0	0	0	3.005			
S_7	0	0	0	0	0	0.589	0.674		
S_8	0	0	0	0	0	0	0	0.804	
S_9	0	0	0	0	0	0	0	0.038	5.020

TABLE 5: Comparison of Calculated and Experimental IR Frequencies (cm^{-1}) and Assignmentss[a]

no.	symmetry type	band type	expt (this work)	calc	assignment[a]	
1	A_1	B	(282)[b]	291	$S_1(86)$	CCl_2 scissors
2	A_1	B	715	707	$S_2(80)$	C−Cl symm stretch
3	A_1	B	(1434)[b]	1430	$S_3(99)$	CH_2 scissors
4	A_1	B	2997	2986	$S_4(100)$	CH symm stretch
5	A_2		(1153)[b]	1159	$S_5(100)$	twist
6	B_2	A	760	767	$S_6(92)$	CCl asymm stretch
7	B_2	A	1270	1277	$S_7(98)$	CH_2 wagging
8	B_1	C	898	880	$S_8(100)$	CH_2 rocking
9	B_1	C	3068	3070	$S_9(100)$	CH asymm stretch

[a] See Table 2 for definition of S_i. [b] Taken from Raman data reported by Escribano et al.[5]

TABLE 6: Comparison of Calculated and Experimental IR Intensities ($\times 10^6$ cm mol^{-1})

no.	expt freq (cm^{-1})	gas-phase intensity[a]	calc intensity[a]	expt liquid intensity[b]
1	282		0.09	1.92
2	715	1.0	1.87	1.99
3	1434	0.025	0.01	0.38
4	2997	0.71	0.71	0.19
5	1153	0	0	0
6	760	11.3	14.7	12.32
7	1270	3.1	5.27	2.88
8	898	0.07	0.18	0.38
9	3068	<0.01	0.01	0.45

[a] This work. [b] Reference 27.

The Self-Consistent Molecular Model

Rotational, B_0, constants are available from Davis et al.[4] and Myerst et al.[33] The force field (Table 4) was used to calculate B_z-B_0 corrections, which account for vibration−rotation interactions. Centrifugal distortions and corrections arising from electronic contributions were ignored, as well as isotope effects on the geometry and the force field. With these corrections the B_0 values can be converted to B_z ($\approx B_\alpha^0$) values, which are needed in a joint microwave electron diffraction analysis. The results are given in Table 7. Once the microwave data are brought to the r_α^0 basis, one needs to bring the electron diffraction r_a distances to the same basis by eliminating vibrational effects, i.e. by applying shrinkage corrections, $r_a - r_\alpha^0$. These corrections are well described[34] and given by

$$r_a - r_\alpha^{\,0} = K^0 - U^2/r_a \qquad (6)$$

K^0 represents the vibrational amplitude perpendicular to the internuclear distance. Its value is calculated along with the mean vibrational amplitude U from the harmonic force field (Table

TABLE 7: Experimental Rotational Constants B_0, Corrections $B_z - B_0$ Required for Harmonic Vibrational Interactions, and the Resulting B_z Values To Be Compared with B_α^0 Values Derived from the Joint Microwave Electron Diffraction Data[a]

	B_0 (cm^{-1})	$B_0 - B_z$ (cm^{-1})	B_z (cm^{-1})	B_α^0 (cm^{-1})
		$CH_2Cl(35)Cl(35)$[a]		
A	1.067 481	0.005 243(786)	1.062 238(786)	1.062 610
B	0.110 753	0.000 140(21)	0.110 613(21)	0.110 630
C	0.102 245	0.000 075(11)	0.102 170(11)	0.102 181
		$CH_2Cl(35)Cl(37)$[b]		
A	1.063 343	0.005 243(786)	1.058 100(786)	1.058 505
B	0.107 791	0.000 140(21)	0.107 651(21)	0.107 659
C	0.099 676	0.000 075(11)	0.099 601(11)	0.099 604
		$CH_2Cl(37)Cl(37)$[b]		
A	1.059 20	0.005 243(786)	1.053 957(786)	1.054 380
B	0.104 84	0.000 140 (21)	0.104 700(21)	0.140 710
C	0.097 134	0.000 076(11)	0.097 058(11)	0.097 044

[a] Taken from ref 4. [b] Taken from ref 3.

TABLE 8: Calculated Vibrational Amplitudes U, Perpendicular Amplitudes K^0, and Shrinkage Corrections $K^0 - U^2/r_a$ (all in Å × 1000)

	U	K^0	$K^0 - U^2/r_a$
C−H	77	14	8
C−Cl	51	1	−0.5
H···H	123	15	7
H···Cl	108	5	0
Cl···Cl	71	0	−2

4).[2,24] Table 8 summarizes the K^0 and U values and the shrinkages for the distances.

In order to combine the diffraction intensities with the microwave rotational constants a proper weighting scheme is needed. Weights for the diffraction data were chosen to be proportional to s and were scaled down at each end of an s interval.[11] Rotational B_z data were given a weight $w = k/\epsilon^2$ relative to the diffraction data; k is commonly chosen as 10^{-5} while ϵ (the estimated error) is taken as 15% of the $B_z - B_0$ correction. This led to weights of 16 for the A, 2×10^4 for the B, and 8×10^4 for the C rotational constants.

A least-squares refinement was performed on these data refining the four geometrical parameters, three indices of resolution, and one scale factor ($k(U)$) on the vibrational amplitudes. This means that we fixed the thermal parameters U_{ij} to the calculated values (Table 8). Since the force field (Table 4) reproduces the IR frequencies with an accuracy of about 1%, the calculated electron diffraction thermal parameters also have an accuracy of about 1%, which surpasses the accuracy that would emerge from a least-squares analyses of the electron diffraction data. Furthermore, the scale factor $k(U)$ is used to correct for the difference (if any) between the actual temperature of the diffracting molecules and the temperature taken in the calculations (300 K). Conversely, when U parameters are fixed to the calculated values, $k(U)$ measures the quality of the electron diffraction data set together with the indices of resolution. The closer to unity these indicator parameters are, the better the data set. Tables 9 and 10 show the results.

To test the above strategy, we added three U values to the list of refinable parameters and repeated the least-squares analysis. Significant changes were noted neither in the disagreement factors, R, nor in the final geometrical and thermal parameters.

Although only the C−Cl and H···H distances overlap (see Figure 4), the correlation coefficients (Table 10) between the geometrical parameters are high. This is due to the fact that the molecule has C_{2v} symmetry with quasi-tetrahedral angles; it is not a sign of a possibly incorrect model choice.

TABLE 9: Results of Least-Squares Refinement. Esd Values Given in Parentheses Are Multiplied by 3 and Refer to the Last Digit

Geometrical Parameters		
	r_α^0 basis	r_g basis
r_1 (C−H) (Å)	1.090(10)	1.104(10)
r_2 (C−Cl) (Å)	1.772(2)	1.773(2)
θ_1 (H−C−H) (deg)	112.0(1.0)	
θ_2 (Cl−C−Cl) (deg)	112.0(0.1)	
Indices of Resolution		
k_1 (60 cm)	0.99(3)	
k_2 (35 cm)	0.95(5)	
k_3 (20 cm)	0.92(12)	
Scale Factor on Vibrational Amplitudes		
$k(U)$	0.99(8)	
Disagreement Factors[a]		
R(ED)	0.001 850	
R(MW)	0.000 126	
R(total)	0.000 826	

[a] R values are defined as $R = [\sum w(I_{obs} - I_{calc})^2/\sum w I_{obs}^2]^{1/2}$, with I representing ED (electron diffraction) intensities or MW (microwave) constants, and w signifying weight factors (see Self-Consistent Molecular Model section).

TABLE 10: Correlation Coefficients (×100) among Parameters

	r_1	r_2	θ_1	θ_2	$k(U)$	k_1	k_2	k_3
r_1	100							
r_2	−73	100						
θ_1	−18	74	100					
θ_2	−75	79	71	100				
$k(U)$	−1	3	4	3	100			
k_1	−4	9	9	8	59	100		
k_2	−4	7	7	7	70	42	100	
k_3	0	2	3	2	65	39	46	100

The most interesting as well as the most accurate geometrical parameter is the C−Cl bond length. Mostly due to Kuchitsu and his co-workers,[34−37] the various existing distance types can be converted into one another by eqs 6−8:

$$r_g = r_e + (3\alpha/2)U^2 \tag{7}$$

$$r_z \approx r_\alpha^0 = r_e + (3\alpha/2)U^2 - K^0 \tag{8}$$

Here, α is the Morse anharmonicity parameter normally estimated from an appropriate diatomic molecule. Taking α-(CCl) = 1.90 Å^{-1} [38] with the calculated thermal parameters (Table 8), we obtain r_e(CCl, expt) = 1.765 Å, which shows that the 6-31G* calculated r_e(CCl; 6-31G*) overestimates the experiment by 0.013 Å in CH_2Cl_2. Interestingly, Dobbs and Hehre[39] found in CH_3Cl that r_e(CCl, 6-31G*) overestimates r_g-(CCl, expt) by 0.004 Å. The comparison of ab initio bond lengths with gas-phase experimental ones is often performed at the r_g level with the help of empirical $r_g - r_e$ corrections.[40−42] These corrections simultaneously eliminate the basis set artifacts and introduce the anharmonicity of the real vibration. From the present work it follows that for C−Cl the $r_g - r_e$(6-31G*) correction is estimated as −0.004 Å and the $r_g - r_e$(4-21G*) correction as −0.015 Å.

Beagley[43] has pointed out that the C−F bond lengths in the series $CH_{4-n}F_n$ ($n = 1-4$) decrease steadily from 1.38 to 1.32 Å as extra fluorine atoms are attached to carbon as a result of the strong electronegativity of fluorine. For the other halogen series the trends are less clear. Chadwick and Millen[44] discussed inter alia the chlorine series, but did not compare C−Cl lengths of the same type, i.e. they compared r_s bond lengths with r_g

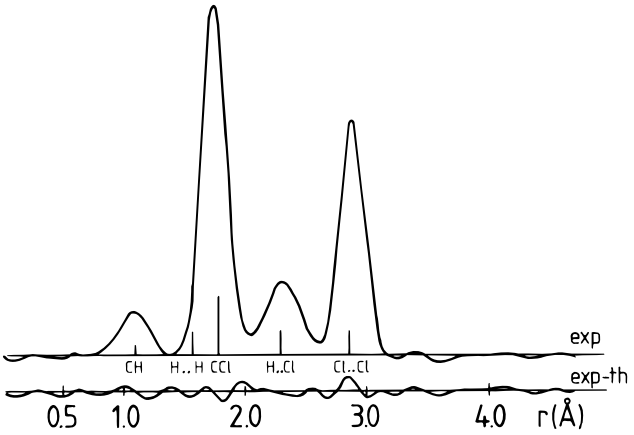

Figure 4. Experimental radial distribution function of CH_2Cl_2 (upper curve). A damping factor of exp(−0.002) s^2 was used. Distances are indicated by vertical bars of length proportional to $n_{ij}(Z_iZ_j/r_{ij})$, in which Z_i denotes the atomic number of atom i, r_{ij} the distance between atoms i and j, and n_{ij} the number of times r_{ij} occurs in the molecule. The difference curve (lower) is given as experimental results − theoretical results.

TABLE 11: Experimental Carbon−Chlorine Bond Lengths, Converted to r_α^0 Geometry, in Gaseous $CH_{4-n}Cl_n$ ($n = 1-4$) with esd's in Parentheses

	r_α^0 (Å)	ref		r_α^0 (Å)	ref
CH_3Cl	1.786(4)	45	$CHCl_3$	1.761(−)	46
CH_2Cl_2	1.772(2)	this work	CCl_4	1.766(3)	47

bond lengths. The trend becomes clear when one converts (eqs 6−8) the published C−Cl lengths to the r_α^0 level, using U(C−Cl) = 0.051 Å and K^0(CCl) = −0.0005 Å throughout the series. The extra uncertainty thus introduced is estimated to be 0.001 Å and is accounted for in the estimated standard deviation (esd) values quoted for the resulting r_α^0 values shown in Table 11. The C−Cl distance decreases steadily from CH_3Cl to CH_2Cl_2 and to $CHCl_3$, but not so strongly as in the fluoromethanes because of the smaller electronegativity of chlorine compared to that of fluorine. Addition of the fourth chlorine causes a slight increase in the bond length due to the increasing influence of steric hindrance. Thus, in the halogenomethanes the C−Hal bond length is governed by the competing effects of electronegativity (shortening) and steric hindrance (lengthening), causing the C−F length to decrease whereas the C−I length is expected to increase in the series $CH_{4-n}X_n$.

Acknowledgment. C.V.A. acknowledges support as a research director by the Fund for Scientific Research-Flanders, FWO. J.D.S. thanks the Belgian Organization IWONL for a predoctoral grant. J.T. is grateful to NFWO for a visiting professorship. Financial aid to the laboratory by DPWB (Information Technology, part Supercomputing; contract IT/SC/23) is gratefully acknowledged. This paper represents results of the Belgian Programme on Interuniversity Attraction Poles initiated by the Belgian State - Prime Minister's Office - Science Policy Programming. Scientific responsibility is assumed by the authors.

References and Notes

(1) Aroca, F.; Robinson, E. A.; Ford, T. A. *J. Mol. Struct.* **1976**, *31*, 177−185.

(2) Wilson, E. B.; Decius, J. C.; Cross, P. C. *Molecular Vibrations, The Theory of Infrared and Raman Vibrational Spectra*; McGraw-Hill: New York, 1955; pp 177−178.

(3) Wang, Y.; De Smedt, J.; Coucke, I.; Van Alsenoy, C.; Geise, H. J. *J. Mol. Struct.* **1993**, *299*, 43.

(4) Davis, R. W.; Robiette, A. G.; Gerry, M. C. L. *J. Mol. Spectrosc.* **1981**, *85*, 399−415.

(5) Escribano, R.; Orza, J. M.; Montero, S.; Domingo, C. *Mol. Phys.* **1979**, *37*, 361−377.

(6) Tamagawa, K.; Iijima, T.; Kimura, M. *J. Mol. Struct.* **1976**, *37*, 243−253.

(7) Van Loock, J. F.; Van den Enden, L.; Geise, H. J. *J. Phys. E* **1983**, *16*, 255.

(8) Forster, H. R. *J. Appl. Phys.* **1970**, *41*, 5344.

(9) Bonham, R. A.; Schäfer, L. In *International Tables for X-ray Crystallography*; Kynoch Press: Birmingham, U.K., 1974; Vol. 4, Chapter 2.5.

(10) Tavard, C.; Nicolas, D.; Rouault, M. *J. Chim. Phys., Phys. Chim. Biol.* **1964**, *40*, 1686.

(11) Van den Enden, L.; Van Laere, E.; Geise, H. J.; Mijlhoff, F. C.; Spelbos, A. *Bull. Soc. Chim. Belg.* **1976**, *85*, 735.

(12) Saëki, S.; Tanabe, K. *Spectrochim. Acta* **1969**, *25A*, 1325.

(13) Welsh, H. L.; Crawford, M. F.; Thomas, T. R.; Love, G. R. *Can. J. Phys.* **1952**, *30*, 577.

(14) Pulay, P. *Mol. Phys.* **1969**, *17*, 197.

(15) Pulay, P. In *Modern Theoretical Chemistry*; Schaefer, R. G., III, Ed.; Plenum: New York, 1977; Vol. 4, pp 153 ff.

(16) Peeters, A.; Van Alsenoy, C. *J. Mol. Struct. (THEOCHEM)* **1993**, *286*, 19.

(17) Pulay, P.; Fogarasi, G.; Pang, F.; Boggs, J. E. *J. Am. Chem. Soc.* **1979**, *101*, 2550.

(18) Gordon, M. S.; Binkley, J. S.; Pople, J. A.; Pietro, W. J.; Hehre, W. J. *J. Am. Chem. Soc.* **1982**, *104*, 2797.

(19) Francl, M. M.; Pietro, W. J.; Hehre, W. J.; Binkley, J. S.; Gordon, M. S.; Defrees, D. J.; Pople, J. A. *J. Chem. Phys.* **1982**, *77*, 3654.

(20) Ditchfield, R.; Hehre, W. J.; Pople, J. A. *J. Chem. Phys.* **1971**, *54*, 724.

(21) Hehre, W. J.; Ditchfield, R.; Pople, J. A. *J. Chem. Phys.* **1972**, *21*, 2257.

(22) Pulay, P.; Fogarasi, G.; Boggs, J. E. *J. Chem. Phys.* **1981**, *74*, 3993.

(23) Von Carlowitz, S.; Zeil, W.; Pulay, P.; Boggs, J. E. *J. Mol. Struct.* **1982**, *30*, 113.

(24) Califano, S. *Vibrational States*; Wiley-Interscience: New York, 1976.

(25) Hamilton, W. C. *Statistics in Physical Science*; Ronald Press: New York, 1964; pp 157 ff.

(26) Wilson, E. B.; Decius, J. C.; Cross, P. C. *Molecular Vibrations, The Theory of Infrared and Raman Vibrational Spectra*; McGraw-Hill: New York, 1955; Chapter 7.

(27) Rendell, C. H.; Ford, T. A.; Redshaw, M.; Orville-Thomas, W. J. *J. Mol. Struct.* **1975**, *24*, 187−204.

(28) Evans, J. C.; Lo, G. Y.-S. *Spectrochim. Acta* **1965**, *21*, 33.

(29) Buckingham, A. D. *Proc. R. Soc. Ser. A* **1958**, *258*, 169.

(30) Hirota, E. *Bull. Soc. Chem. Soc. Jpn.* **1954**, *27*, 295.

(31) Ratajczak, H.; Orville-Thomas, W. J. *Trans. Faraday Soc.* **1965**, *61*, 2603.

(32) Polo, S. R.; Wilson, M. K. *J. Chem. Phys.* **1955**, *23*, 2376.

(33) Myerst, R. J.; Gwinn, W. D. *J. Chem. Phys.* **1952**, *20*, 1420.

(34) Kuchitsu, K. In *Molecular Structure and Vibrations;* Cyvin, S. J., Ed.; Elsevier: Amsterdam, 1972; Chapter 12.

(35) Kuchitsu, K. *J. Chem. Phys.* **1968**, *49*, 4456.

(36) Kuchitsu, K.; Fukuyama, T.; Morino, Y. *J. Mol. Struct.* **1968**, *1*, 463.

(37) Kuchitsu, K.; Fukuyama, T.; Morino, Y. *J. Mol. Struct.* **1969**, *4*, 41.

(38) Kuchitsu, K.; Morino, Y. *Bull. Soc. Chem. Jpn.* **1965**, *38*, 805.

(39) Dobbs, K. D.; Hehre, W. J. *J. Comput. Chem.* **1986**, *7*, 359−378.

(40) Schäfer, L.; Van Alsenoy, C.; Scarsdale, J. N. *J. Mol. Struct. (THEOCHEM.)* **1982**, *86*, 349.

(41) Schäfer, L. *J. Mol. Struct.* **1983**, *100*, 51.

(42) Van Alsenoy, C.; Klimkowski, V. J.; Schäfer, L. *J. Mol. Struct. (THEOCHEM.)* **1984**, *109*, 321.

(43) Beagley, B. In *Chemical Society of London, Specialist Periodical Report*; Suton, L. E., Ed.; 1973; Vol. 20, Chapter 2.

(44) Chadwick, D.; Millen, D. J. *J. Mol. Struct.* **1975**, *25*, 216−218.

(45) Bartell, L. S.; Brockway, L. O. *J. Chem. Phys.* **1955**, *23*, 1860.

(46) Cited by Davis et al.[4] as a personal communication from M. Kimura, 1980.

(47) Morino, Y.; Nakamura, Y.; Iijima, T. *J. Chem. Phys.* **1960**, *32*, 643−652.

(48) Shibata, S.; Iijima,K.; Tani, R.; Nakamura, Y. *Rep. Fac. Sci., Shizuoka Univ.* **1974**, *9*, 33.